



Research Article

Acoustic emission signal 'peak amplitude-distribution' analysis related to concrete fracture under uniaxial compression

R. Vidya Sagar *

Department of Civil Engineering, Indian Institute of Science, Bangalore 560 012, India

ABSTRACT

Acoustic emissions (AE) released during the compressive fracture of cementitious materials have been subjected to analysis using 'AE based b -value' to study the fracture process. Identification of the 'AE sources locations' in three dimension is not always possible. With a minimum number of AE sensors mounted on the test specimen and by using the AE based b -value analysis, it is possible to study fracture process and the damage status in solids. The b -value of AE is calculated using the Gutenberg-Richter empirical relationship (G-R law), which is available in seismology. The details related to original G-R relation and its suitability for AE testing were discussed. In this article it has been tried to look into the variations of the AE based b -value in cementitious test specimens prepared with different cementitious mixture proportions. Effect of (i) coarse aggregate size in cementitious materials (ii) loading rate during compressive fracture process (iii) age of concrete on b -value variation were discussed. The trend of variation in AE based b -value during fracture process in concrete and mortar was different. It was observed that when the compression toughness of the cementitious material increases, higher b -values were observed. When the loading rate was high, quick cracking occurred and lower b -values were observed. As the coarse aggregate size in the cementitious material increases, the cumulative AE energy was higher. The reason may be due to the compression toughness of the cementitious material. The AE based b -value is useful to identify the different stages of compressive fracture process in solids.

ARTICLE INFO

Article history:

Received 3 August 2018

Revised 19 September 2018

Accepted 25 September 2018

Keywords:

Non-destructive testing

Concrete

Fracture

Acoustic emission

Uniaxial compression

1. Introduction

Monitoring of crack development in concrete structures *in-situ* is required and also compulsory in case of some structures. For example, in case of pressure vessels, nuclear power plant structures, monitoring of crack initiation, coalescence, propagation more or less required continuously. Because, the potential loss in concrete strength, cracking that might occur with time. Therefore, structural health monitoring (SHM) of concrete structures is necessary. Ageing of concrete structures (residential buildings, public buildings), heavy loads on bridges (due to increasing traffic volume), aggressive environment (acid rains, air-pollution,

and salts) are few causes behind the necessity for the frequent health monitoring of concrete structures. It would, therefore, be useful to have available non-destructive testing (NDT) methods for monitoring concrete structures that is sensitive enough to indicate sufficient warning of an impending collapse of structures. Also to know whether cracks are developed or not in concrete structures under service loads NDT methods are useful (Nair and Cai, 2010; Kalayanasundaram et al., 2007; Holford, 2000). Based on non-destructive testing observations repairs could be made before the damage becomes rigorous.

1.1. Brief introduction to acoustic emission testing

Acoustic emission (AE) testing is a NDT method to monitor fracture process in real time and also to assess the damage status in solids/structures. By using this passive NDT method the active cracks and their characteristics can be studied. The entire concrete structure can be monitored for cracks in a single inspection. The real time progress of fracture process can be studied by mounting minimum required number of AE sensors on the structure (Gross and Ohtsu, 2008; Ohtsu, 1998). During fracture process in solids the strain energy is released in the form

of elastic waves (or stress waves) and reach to the surface of the solid/structure. AE refers to the generation of transient elastic waves during the rapid released of energy from localized sources within a solid (Kalyanasundaram et al., 2007). By mounting the required number of PZT sensors on the test specimen or structure these elastic waves can be recorded. Subsequently, the PZT sensors convert the elastic waves into electrical signals. A schematic representation of a typical AE signal and corresponding parameters are shown in Fig. 1. By using these signals the fracture process occurred in real time can be studied in solids (RILEM TC-ACD, 2012a; 2012b, 2012c).

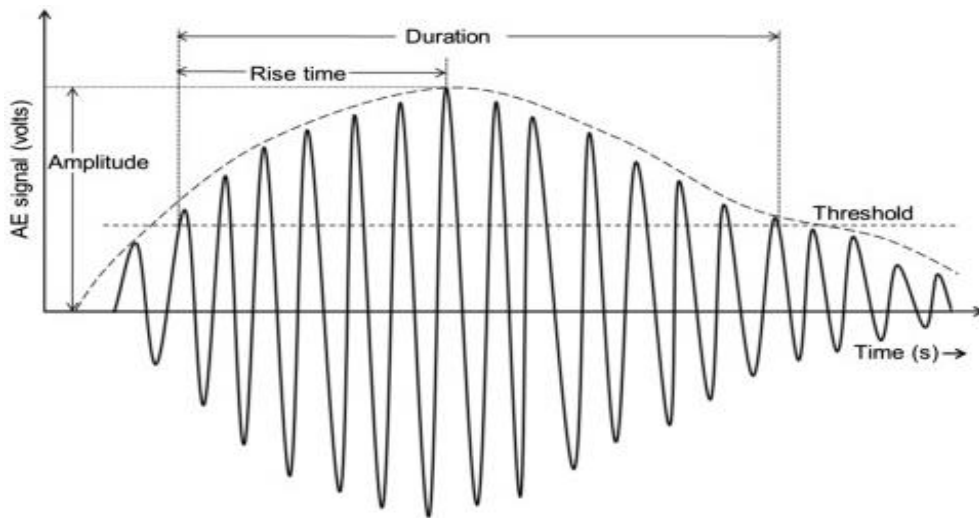


Fig. 1. Schematic representation of an AE signal and corresponding parameters (Datt et al., 2015).

1.2. AE based b-value

Researchers confirmed that there is a close analogy exists between AE produced during fracture process in solids and the seismic waves caused due to earthquake (Rao and Lakshmi, 2005). Analogous to the occurrence of earthquakes, during fracture process in

solids, higher amplitude acoustic emissions (stress waves caused by internal material fracture or micro seismic activity) released less in number and lower amplitude AE more in number as shown in Fig. 2. It can be observed that AE peak amplitudes greater than 60 dB are less when compared with lower amplitude AE hits.

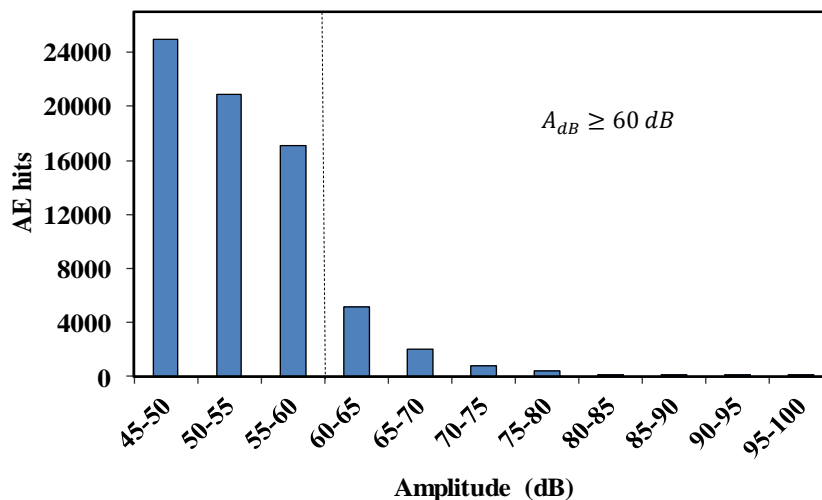


Fig. 2. Distribution of the number of AE hits versus AE peak amplitude.

Also, AE released during fracture process in solids are similar to the P-waves that generated during occurrence of earthquake. Because of similarities between occurrence of earthquakes and happening of AE events during fracture process in solids, researchers attempted to use Gutenberg-Richter law available in seismology (Gutenberg and Richter, 1954; Mogi, 1964). However, researchers modified the Gutenberg-Richter law to study frequency of occurrence-amplitude distribution of AE released during fracture process in solids (Colombo et al., 2003).

$$\log_{10}N(A) = a - b \left[\frac{A_{dB}}{20} \right]. \quad (1)$$

In Eq. (1), A_{dB} is the peak amplitude of the AE (hits or events) in decibels. b is the AE based b -value. $N(A)$ is the number of AE hits of amplitude greater than A . 'a' is constant. The details about Eq. (1) and the theory of "AE based b -value" are discussed in Appendix-A.

2. Literature Review

The AE based b -value is a parameter to study damage status and fracture process in solids (Colombo et al., 2003). This b -value has been used for structure damage evaluation by several researchers. Colombo et al. (2003) studied the variation in the AE based b -values for a reinforced concrete (RC) beam subjected to incremental cyclic loading. The variation in b -values was compared to the micro-cracking and macro-cracking observed during the fracture process. It was concluded that, minimum b -value indicates the formation of macro-cracks and maximum b -value denotes micro-cracking. The AE based b -value analysis has been used for structural damage evaluation by several researchers Shiotani et al. (2001), Kurz et al. (2006), Ko and Yu (2009) Schumacher et al. (2011). Proverbio et al. (2011) assessed damage in post-tension concrete viaduct using b -value analysis and concluded that a decrease in b -value could be an indication of an impending fracture. Schumacher et al. estimated the operating loading on RC highway bridges with b -value analysis. Carpinteri et al. (2006) observed that the AE based b -value ranges from 1.5 to 1.0 when the fracture process progress in the critical state to final collapse. Vidya Sagar and Rao (2014) investigated the effect of loading rate on b -values related to fracture process in reinforced concrete (RC) flanged beams.

Though, AE based b -value was accepted to be a suitable parameter to characterize various stages of fracture process in solids, the studies related to the influence of (i) concrete strength (ii) coarse aggregate size in concrete (iii) rate of loading (iv) curing period of concrete on b -value when concrete is under uniaxial compression are minimum. Lack of complete understanding of AE based b -value, when there is a change in cementitious material mixture proportion, insufficient statistics of experimental data still keeps the AE based b -value analysis problem opened for further discussion. The further work done in this study is that the AE based b -value is used to study fracture process in cementitious materials under uniaxial compression and discussed this useful damage assessment parameter in detail.

3. Research Significance

Characterizing different stages of fracture process in concrete structures using AE testing provide an early warning for any probable damage in concrete structures (Grosse and Ohtsu, 2008; Uchida et al., 2011). It is known that concrete structures are no longer maintenance free. For *in-situ* monitoring of damage in concrete structures, the variation in b -values provides useful information related to micro-cracking and macro-cracking. Since it is not easy to obtain 3-D source location data of high frequency and low amplitude AE. With a minimum required number of AE sensors the fracture process in a concrete structures can be studied using AE based b -value. Concrete structures have many structural components associated with it and the column is one of the most important compression members as it supports the whole structure. In some cases short-columns are required for construction. Uniaxial compression has been important in studying behavior of short columns. The results of the present study lead to understanding of the fracture process in concrete subjected to uniaxial compression and also may be further application of AE testing in structural health monitoring of concrete structures.

4. Experimental Procedure

Unconfined uniaxial compression tests were conducted and monitored the deformation and failure behavior of a set of cement concrete and mortar cylindrical specimens (150 mm diameter and 300 mm height) in Structures Laboratory, Department of Civil Engineering, Indian Institute of Science Bangalore, India. The tests were carried out under displacement control at a constant rate of 0.005 mm/s and 0.002 mm/s using a servo-controlled testing machine (1200 kN capacity, MTS machine) and by recording the released AE simultaneously. The rate of loading is assumed (not as per any standard) to test the samples in the laboratory. This kind of MTS machine is controlled by an electronic closed-loop servo-hydraulic system. It is therefore possible to perform tests under load or displacement control.

4.1. Materials

Three different cementitious materials namely, Concrete-I, Concrete-II and cement mortar were considered in this study. Concrete-I consists maximum coarse aggregate size of 20 mm and its mixture proportion per 1 cubic meter (by mass) was 414:729:1143 (cement: fine aggregates: coarse aggregates). The water/cement (w/c) ratio was 0.46. Concrete-II mixture proportion was 450:716:1100 and its w/c ratio was 0.526. For cement mortar specimens 1343 kg/m³ sand, 285.5 liters water and 543 kg/m³ cement were used. The difference between Concrete-I and Concrete-II is not the maximum grain size of the aggregate alone. water/cement ratio, cement dosage are also different. However, the aim is to study the influence of the coarse aggregate on AE peak amplitude distribution.

4.2. Test specimens

Eleven specimens were cast using each cementitious materials namely, Concrete-I, Concrete-II and Cement mortar (total 31 specimens). Cement mortar specimens were tested to study the coarse aggregate influence on AE characteristics of cement concrete. All specimens were cast in mild steel cylindrical molds with a diameter of 150 mm and height of 300 mm. One end of the steel mold was capped to form a cylinder. Concrete was placed in nearly 100 mm thick layer and immediately compacted. An internal needle vibrator was used to ensure proper compaction of the cementitious mixtures.

Test specimens were kept in the molds for the first 24 hours, with the top surface covered with a wet gunny bag. At the age of 24 hours the specimens were removed from their molds. Specimens were placed in a water tub until the time of testing. Before testing, the specimens were taken out from water tub and kept for drying. The specimens were tested for different curing periods of 7 days, 15 days and 28 days for Concrete-I, 9 days, 17 days and 28 days for Concrete-II and 7 days, 15 days and 28 days for cement mortar. The uniaxial compressive strength of test samples (cylinders) at various curing period for Concrete-I, Concrete-II and Cement mortar is shown in Fig. 3.

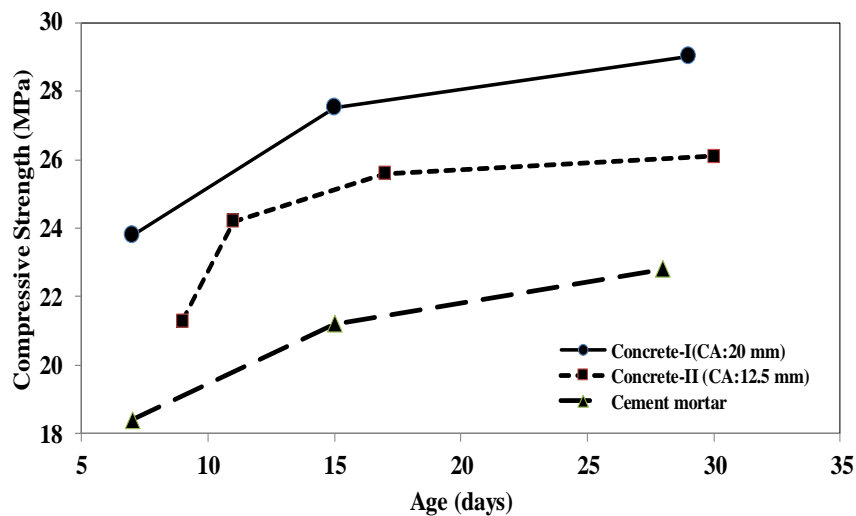


Fig. 3. Compressive strength (cylinder) variation in the three cementitious materials with age.

4.3. AE recording system

The AE signal parameters were recorded via the AE monitoring system during the uniaxial compression of the cementitious materials because the time history of the AE characteristic parameters reflect how fracture process occur and evolve. For AE signal detection, two resonant type differential AE sensors (57 kHz) with pre-amplifier gain of 40 dB were used. The use of two AE sensors is usual for monitoring the AE parameters in laboratory. In this study, recording of AE event locations is not attempted. The AE monitoring system was manufactured by Physical Acoustic Corporation (PAC) NJ, USA. AE^{WIN} SAMOS software and R6D resonant sensors were used. Each AE sensor was attached to the surface of the specimen at a height of 150 mm from bottom of cylinder on either sides of the specimen. The sensor surface was 17.5 mm in diameter and 16.25 mm in height. The surface of the test specimen was thoroughly cleaned and vacuum silicon grease was used as a couplant to both sensor surface and area of sensor location on the test specimen. Brown color gum tape was used to attach the sensor to test specimen and also to apply pressure on sensor to maintain their contact with specimen's surface. A threshold of 40 dB was set to screen out surrounding noise and the AE activity generated due to friction between the top and bottom surface of the specimen with

end plates. AE monitoring system parameters, namely, PDT is 200 μ s, HDT is 400 μ s, HLT is 500 μ s and for maximum duration 1000 μ s were set. The AE data acquisition system was setup to acquire AE signal parameters namely, hits, peak amplitude, counts, energy, duration, signal strength, absolute energy, time, average frequency. The experimental setup is shown in Fig. 4(a). In this study, two AE sensors were mounted on the test specimen as shown schematically in Fig. 4(b).

Fig. 4(c) indicates the optimal frequency response of used AE sensor. It can be observed that at 54.7 kHz frequency the sensors had highest sensitivity at 77.1 dB amplitude. In other words, sensitivity stands for least measurable physical parameter. The AE sensor has a sensitivity and frequency response over the range of 35 kHz - 100 kHz. The peak load, rate of loading, age of concrete and AE parameters namely, counts and energy recorded for all test specimens were shown in Table 1.

5. Procedure to Compute AE based *b*-value

5.1. AE amplitude distributions related to concrete under uniaxial compression

Fig. 5 shows cumulative number of AE hits on the Y-axis (log scale) and amplitude of AE in dB on the X-axis. All the

AE signals were found to fall in the amplitude range of 40 dB to 100 dB. A large number of AE hits had smaller amplitudes and the distribution shows a descending gradient. The slope of the 'linear descending branch' of the cumulative

distribution graph is known as the "AE based b -value". There is a marked change in the trend of the amplitude distribution after the onset of micro cracking in the Concrete-I test samples at $\sim 20\%$ failure stress (σ_f) as shown in Fig. 5.

Table 1. Test specimen details, rate of loading and recorded peak load and AE parameters.

Cementitious material	Age (days)	Specimen	Peak load (kN)	Rate of loading (micron/s)	Total AE counts	Total AE energy (Volt-s)	Time duration of the test (s)
Concrete-I	7	C1_7A	401.1	5			730
		C1_7B	438.9	5	542457	3301627	354
		C1_7C	424.2	5	874633	6630822	804
	15	C1_15A	435.3	5	383468	2708549	860
		C1_15B	587.1	5	355480	1870588	708
		C1_15C	439.1	5	416198	4379934	804
	29	C1_29A	456.3	5	502290	4877430	460
		C1_29B	523.1	5	479272	4612799	780
		C1_29C	337.3	5	985818	8059748	1265
		C1_29D	640.9	5	360657	3359106	540
C1_29E		606.3	5	257030	3221477	470	
Concrete-II	9	C2_9A	378.1	5	327670	870482	863
		C2_9B	378.6	5	694363	2464721	1112
		C2_9C	377.5	5	583085	2934222	954
	11	C2_11A	385.4	5	599407	3794971	830
		C2_11B	471.6	5	348349	3195094	710
	17	C2_17A	407.1	5	90567	2254411	860
		C2_17B	498.7	5	114719	3294762	840
	30	C2_30A	461.9	2	225574	2385511	2238
C2_30B		452.6	5	89919	1654119	876	
Cement Mortar	7	M_7A	336.8	5	216273	854441	624
		M_7B	299.0	5	300999	1178567	714
		M_7C	341.3	5	276197	1074503	642
	15	M_15A	408.8	5	395938	2495569	774
		M_15B	346.75	5	360429	2307427	684
		M_15C	367.4	5	378386	2433103	684
	28	M_28A	438.6	2	465076	1932337	1788
		M_28B	346.2	2	398123	1192909	2550
		M_28C	349.9	5	304666	1283757	805
		M_28D	406.7	5	348197	1011627	730
		M_28E	459.6	5	262887	1370554	790

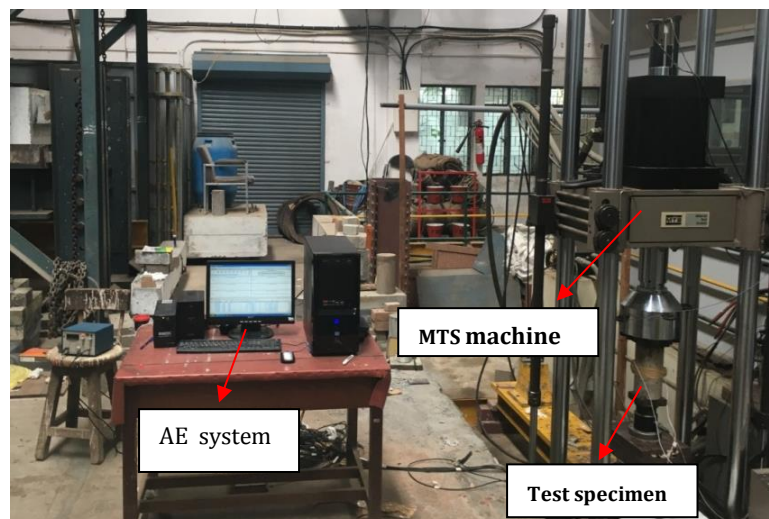


Fig. 4(a). Experimental setup in Structures Laboratory, Department of Civil Engineering, Indian Institute of Science Bangalore, India.

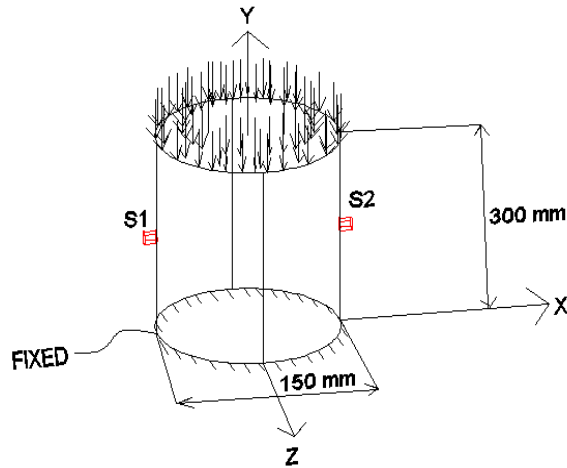


Fig. 4(b). Schematic diagram of the test specimen in isometric view (S1&S2 indicates AE sensors).

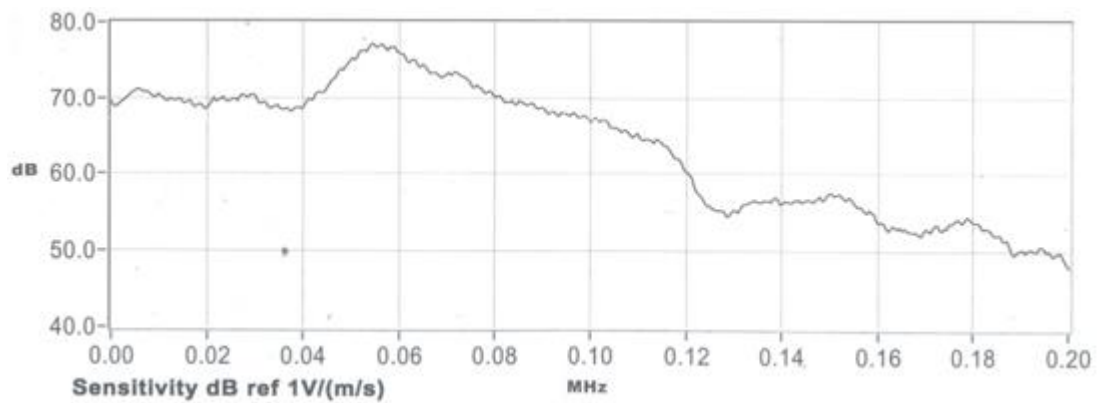


Fig. 4(c). Frequency response of the used AE sensor as given by the manufacturer of AE system. Resonant type AE sensor’s frequency characteristics, maximum amplitude 77.1 dB recorded at peak frequency 54.7 kHz (PAC, AE^{WIN} SAMOS user manual, 2005).

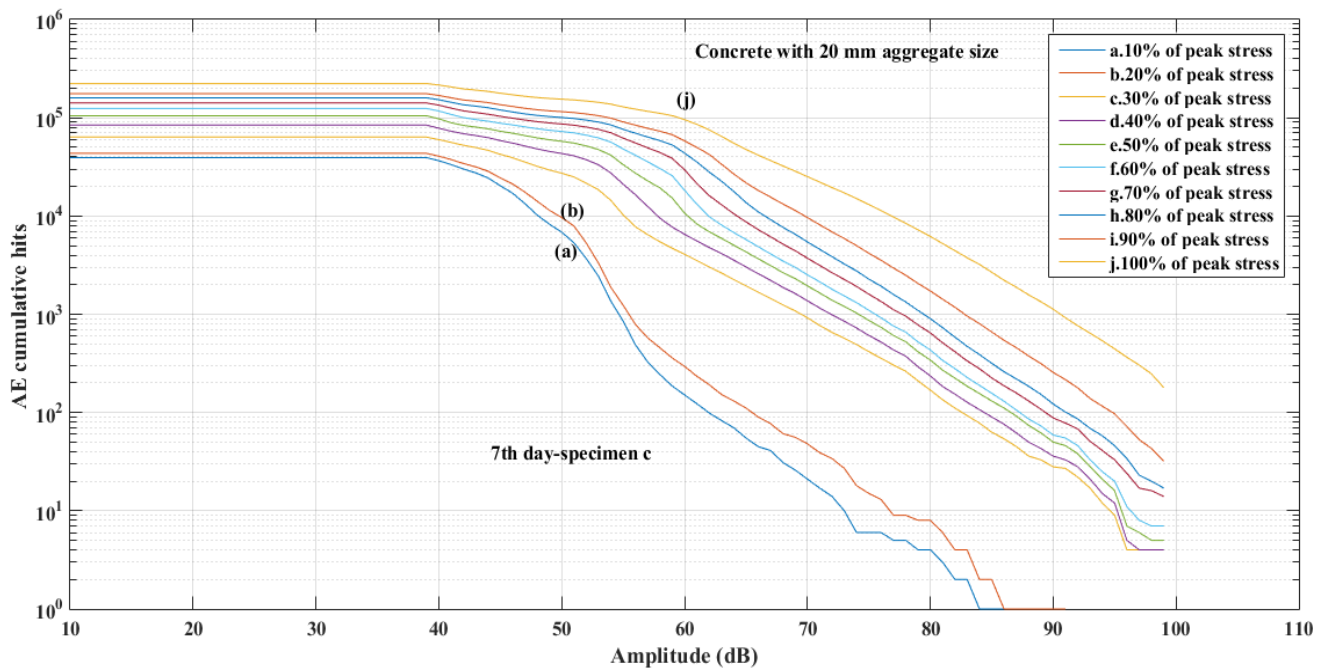


Fig. 5. AE cumulative frequency of occurrence–amplitude distribution graphs corresponding to different stress ranges. The graphs were obtained from the AE recorded during deformation and progressive failure of Concrete-I test specimen under uniaxial compression (Rao and Lakshmi, 2005).

The change of slope of the line plotted between AE cumulative hits and amplitude (also known as *b*-value) indicates the occurrence of fracture process in the solid. From Fig. 5, it can be observed that as the external force applied on the test specimen increases the slope of the line changes as observed in lines (a)-(j) in Fig. 5.

5.2. AE magnitude variation with external stress

Plot between AE frequencies of occurrence-amplitude distributions does not show a single straight line, and different ranges of amplitude indicated different lines. This can be observed in Fig. 6, where a three sets of ‘cumulative AE magnitude distribution’ graphs are shown after applying the necessary correction to convert AE amplitude to magnitude. In the initial stages of compressive fracture process when the stress range is low (0–

20% of σ_f) the AE population is less, the cumulative AE hit-magnitude distribution plot is almost linear. Whereas in the higher stress ranges, the cumulative AE hit magnitude distribution graph shows a ‘fairly good linear relationship’ in the magnitude range from 2.90 to 4.40, although the polynomial fit yields better correlation (Fig. 6). AE frequency of occurrence-magnitude distribution is linear during early stages of loading and appears polynomial curve at stresses near failure as shown in Fig. 6. However, the distribution graph shows a ‘fairly good linear relationship’ in the magnitude range from 2.7 to 4.4.

By following Colombo et al. (2003), the AE based *b*-value was computed. Using Fig. 7 number of hits for group was determined. The cumulative frequency of occurrence - amplitude distribution graphs have been obtained using a Matlab program.

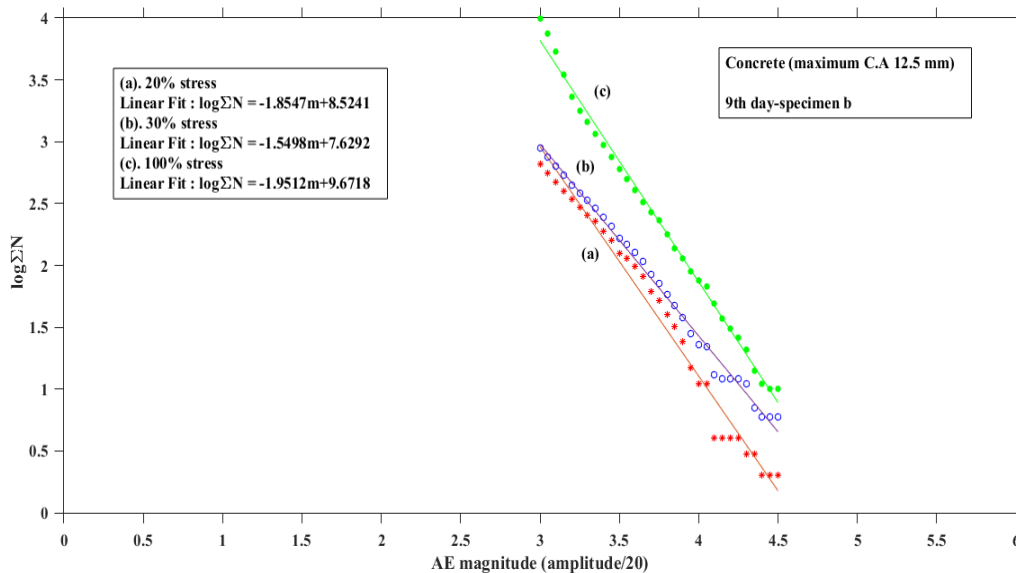


Fig. 6. Cumulative frequency of occurrence-magnitude distribution plots of AE corresponding to three stress ranges (Rao and Laskhmi, 2005).

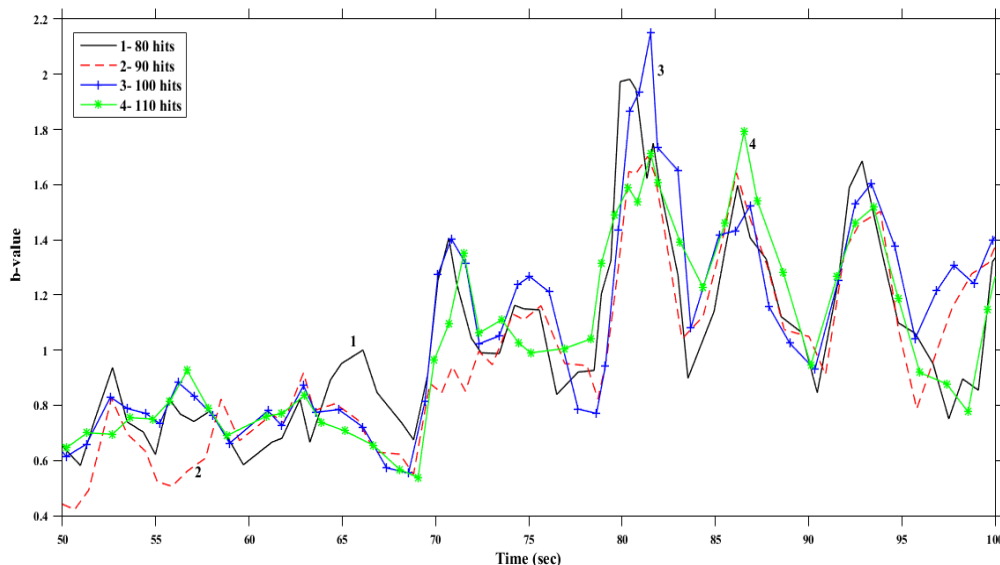


Fig. 7. AE based *b*-value variation with time. *b*-value was calculated using (i) group of 80 hits, (ii) group of 90 hits (iii) group of 100 hits, and (iv) group of 110 hits (Colombo et al, 2003).

6. Results and Discussion

6.1. AE based b -value variation related to cement concrete under uniaxial compression

The variation of b -values versus load and time is shown in Fig. 8. It is observed that a sharp changes in b -value corresponding to the various stages such as formation and growth of stable cracks, crack coalescence and unstable cracks during fracture process. During the early stages of loading (stage-I), AE released due to the closure and rubbing of pre-existing micro-cracks in the concrete began to show a high b -value. A sudden dip in b -value indicates the dominance of AE events of larger amplitude at that time.

Micro cracks are present in a concrete specimen. These cracks may be present due to differential temperatures from hydration, differential drying, and excessive bleeding of water near aggregates. Even before the application of load on the specimen micro cracks are present in the interfacial transition zone (ITZ) between mortar matrix and coarse aggregate (Neville, 2011; vanMier 1997). Cracks in ITZ are formed at boundary of coarse aggregate and mortar matrix due to flow of soft matrix around coarse aggregate. Lateral deformation in matrix is much higher than that in aggregate. This unevenness causes development of shear stresses on top and below of coarse aggregates. In stiff aggregates these stresses lead to formation of shear cones, whose occurrence has been confirmed by many researchers. In case of light weight aggregates instead of going around the aggregates cracks go through them, so tensile splitting prevails (vanMier, 1998).

According Mehta (2006), in the 1st stage, from start of the test to till 30% of peak stress (σ_f) interfacial cracks

remain stable. However, until about 50% of σ_f , a stable system of micro cracks appears to exist in the ITZ. This is Stage -II and at this stage the matrix cracking is negligible. At 50% to 60% of σ_f , cracks begin to form in the cement matrix. With further increase in uniaxial stress to 75% of σ_f , not only does the crack in the ITZ becomes unstable but also the creation and propagation of cracks in the cement matrix increases, causing the stress-strain curve to bend considerably toward the horizontal. This is Stage-III.

At 75% to 80% of σ_f , the rate of 'strain energy release' seems to reach the critical level necessary for crack growth under sustained stress, and the concrete material strains to failure. In short, above 75 % of σ_f , with increasing stress very high strains are developed. This indicates that the crack is becoming continuous due to the rapid propagation of cracks in both the cement matrix and the ITZ. This is the final stage (Stage-IV).

In near peak region the cracks are large and remain stable only when certain conditions are met. At around 80-90% of σ_f , there comes a point where the volume of the specimen becomes minimum. It is because till this point crack opening in lateral direction is less. Beyond this point volume starts to increase; lateral cracks opening becomes so large that effect of axial compression is overcome. Early researchers believed this point of minimum volume as onset of global failure. This is where cracking becomes unstable and collapse is endemic. At the ends of specimen a triaxially confined region is developed due to end platen restraint. For specimen with height to diameter ratio less than 2 this effect is dominant. For ratio greater than 2 this effect is less. For such specimen the specimen can fail along inclined shear crack (high end friction) or through tensile splitting both (vanMier, 1998).

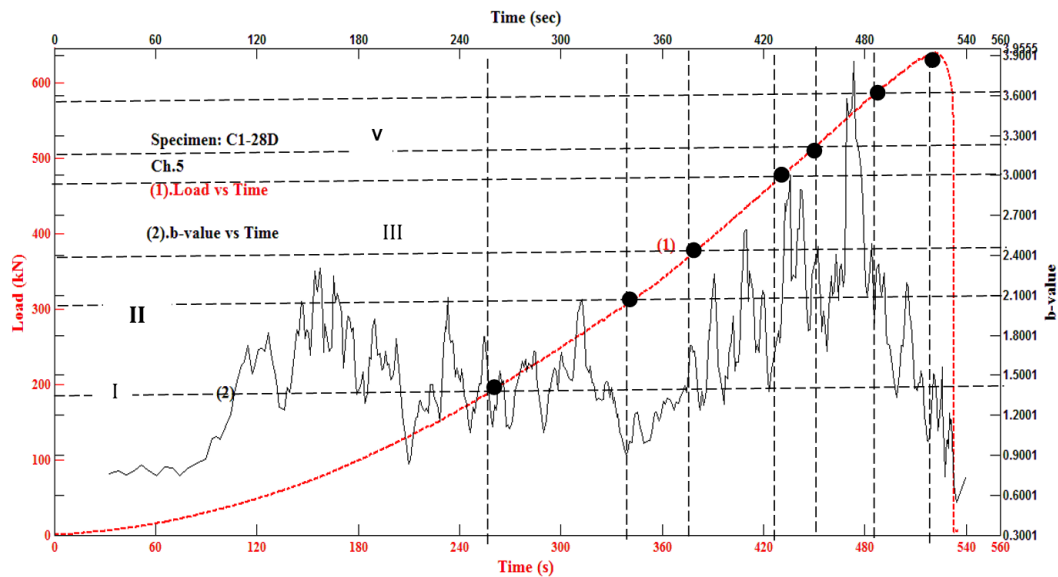


Fig. 8. AE based b -value variation with uniaxial compression load (Specimen; C1-29D, Ch-5).

The presence of sudden decrease in variation in b -value is because of the cracks had started to develop. There could be higher amplitude events in less number occurred. From stage 1 to stage-II, AE based b -value

started to decrease due to high amplitude events occurred at the end of that stage-I, inelastic volume change begins due to the formation of a large number of new micro-cracks. At around 80% of σ_f , the test specimen's volume

is minimum (vanMier, 1998). In other words, the sum of axial stains and lateral strain will decrease. It is observed that at $\sim 80\%$ of σ_f , b -value decreasing sharply to 1.15. With further increase in stress, the b -value increased slightly, marking the transition from 'formation' to 'growth' stage of the newly formed cracks. After 80-90% of σ_f , the test specimen dilated and the lateral cracks has become large that the specimen's volume started to increase. Then it was followed by the onset of unstable cracking as a result of which the b -value decreased until the stress reached a value of 98% failure stress. The coalescence of cracks commenced at this stage. Then the b -value began to decrease sharply due to crack coalescence

and the accompanying stress relief, and at the final failure they had fallen to as low. The newly formed cracks began to grow stably in number and size and the b -value is decreased further until 100 % failure stress. The various stages of compressive fracture and the corresponding b -values are summarized in Table 2. Fig. 9 shows the variation of AE based b -value at different curing days. It can be observed that the 'sudden decrease' occurred in b -value at different percentage of peak compressive stress (σ_{ff}). By the chosen displacement rate as shown in Table-1, the specimen failed in a brittle manner, where the linear branch extends over almost the entire duration of the test.

Table 2. Various stages of compression fracture process and corresponding b -values.

Stage	Stress range	Compression fracture process	AE based b -value
I	0-30% σ_f	Due to short term loading the micro cracks present in ITZ are undisturbed.	1.4
II	30-50% σ_f	Micro cracks starts appear in the ITZ, cement-matrix cracking negligible	1.2
III	50-60% σ_f	Micro cracks begin to form in the cement matrix	1.3
	50-75% σ_f	The crack system becomes unstable in ITZ.	
	60-75% σ_f	Cracks in ITZ becomes unstable, proliferation and propagation of cracks in cement matrix increases	1.7
IV	75-80% σ_f	Release of strain energy reach critical state and cracks becomes unstable. The stress level equals and greater than 75% σ_f is called critical stress.	1.7
V	80-90% σ_f	Volume of the specimen becomes minimum, onset of global failure of a test specimen	1.5
VI	90-100% σ_f	Stress remains constant and strain starts increasing	0.6

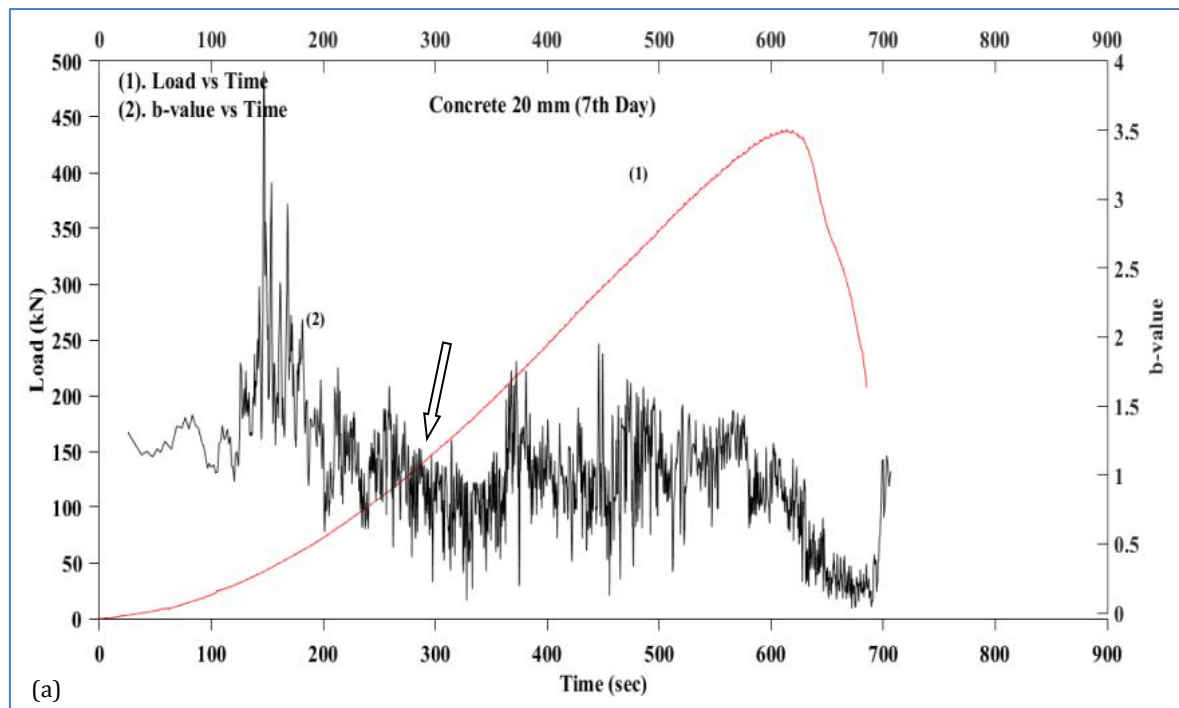


Fig. 9. (continued)

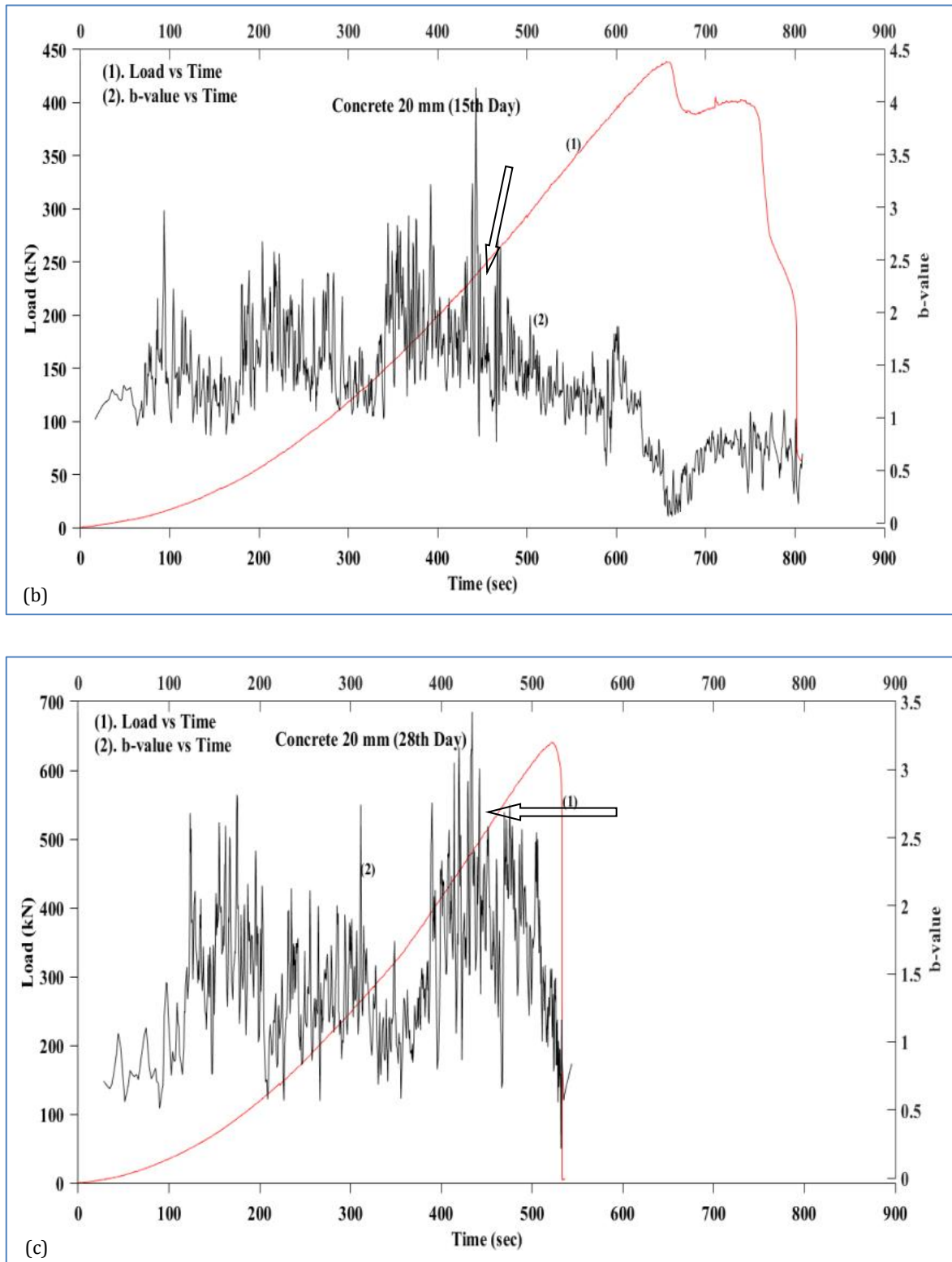


Fig. 9. AE based *b*-value variation with time at age: (a) 7 days; (b) 15 days; (c) 28 days [Concrete-I specimen] (*b*-value was computed for the total AE data recorded by both channels).

Fig. 10 shows the variation of *b*-value with time. The *b*-values were computed at curing periods of 7 days, 15 days and 28 days respectively. It is observed that *b*-values are low for concrete-I at age of 28 days, when compared with *b*-values of concrete with 7 days age. It can be observed from Fig. 3, that the compressive strengths (cylinder) range varies from 18 MPa to 22 MPa for cement

mortar, 21 MPa to 25 MPa for concrete-II and 23 MPa to 29 MPa for concrete-I. The rather high variability in compressive strengths may have been due to variations in the concrete mixture proportions. Therefore, as the strength of the concrete is increasing high amplitude AE events are occurred. The number of high amplitudes events are less, hence the AE based *b*- values is low.

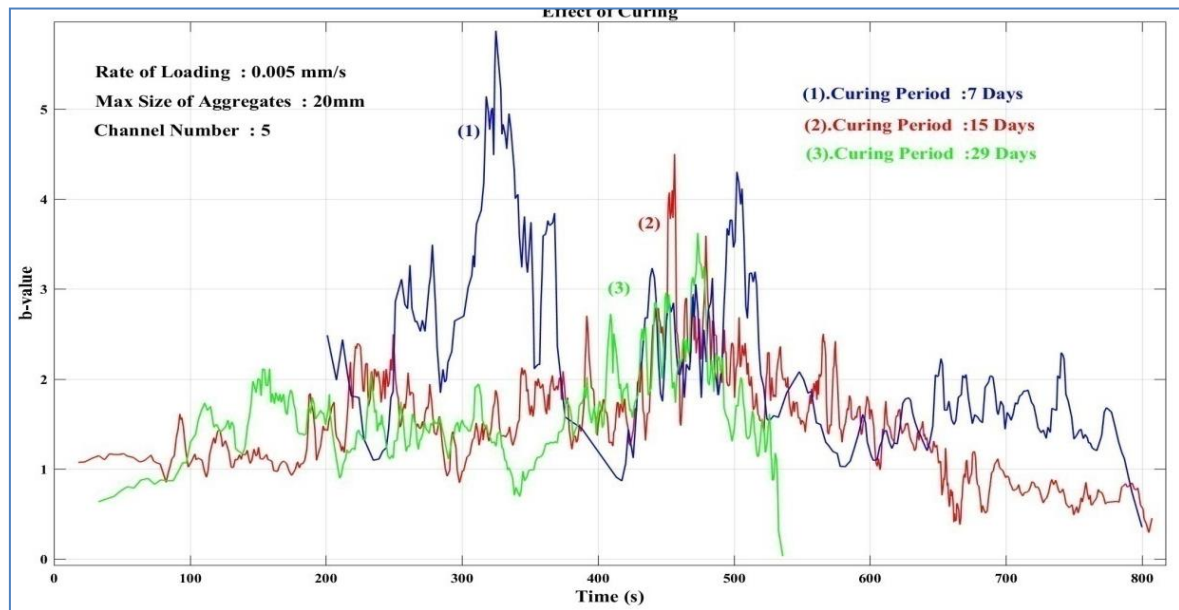


Fig. 10. Influence of curing period on AE based b -value.

6.2. Variation of AE based b -value with sensor location

It is observed that b -value is varying from channel to channel as shown in Fig. 11. This is due to different mechanisms or different degrees of deterioration present in the different zones or locations in the test specimen. The zone or area with the most advanced deterioration to have the lowest b -values.

6.3. Influence of loading rate on AE based b -value related to uniaxial compression of cementitious materials

From Fig.12 it is observed that the AE b -values are low for the specimen tested with high rate of loading. This may be due to release of high amplitude AE events. Higher AE activity such as large number of AE events per time and higher intensity events are observed around the peak load. These observations further prove that the instance of damage initiation is predicted by the lowest b -value. Low b -value may be due to initiation of micro-cracks and cracks opening. Rate of loading can accelerate the micro crack damage which is accompanied by the release of AE. If the rate of loading is too fast (more than what is suggested by the ASTM), there can be a surge or heavy rush of AE. The fluctuations in the b -value variation is more when the rate of loading is high.

AE signals experience attenuation during fracture process in concrete structures, and for that matter in any other imperfect or quasi-brittle materials. Attenuation of AE may be due to heterogeneity of the material as well as micro cracking. A change in the volume of the specimen causes a change in the propagation path length from the crack to the AE sensor, which may affect the recorded AE amplitude. Both the AE amplitude and AE energy as well as the number of AE would be affected uniformly by it weak or strong. In this present study authors invariably

use the number as well as AE amplitude for computing the b -value. Therefore, it should not be an issue since both low amplitude and high amplitude of AE are considered to study the fracture process.

When the loading rate is faster, quick cracking development lead to sudden fluctuations in the b -value at higher loads. Since the concrete behaves relatively more brittle at higher loading rates (or at higher strain rates), the b -values are lower in an average as a few and stronger cracking AE events are created, in contrast to more and weaker cracking events for low rate of loading.

6.4. Influence of coarse aggregate size on released AE

Fig. 13 shows the variation of AE based b -value with time for concrete-II and cement mortar specimens cured for 28 days. When compared b -values of concrete with mortar, low b -values are observed for concrete. The reason could be during fracture process in concrete, high amplitude events in less number are released. A decrease in b -value is seen due to material damage (micro-cracking and macro-cracking) while b -value show a rising trend due to toughening mechanisms like coarse aggregate interlocking, tortuosity of crack path. It is known that AE events are related to cracking. These events are recorded by PZT sensors as electrical signals. And these signals are decayed sinusoidal waves by nature. The number of cycles occurring in unit time in the signal is known as frequency of AE. The "frequency range of the source event" is dependent on its "event duration" (inverse relationship). That is, the source event has a 'broadband spectrum' extending upwards from zero frequency, and starting to decline at a frequency that is inversely proportional to its time duration. This source event duration (t_{ed}) is different from the resulting signal duration (t_{sd}). During fracture process t_{ed} could be different in cement mortar compared with concrete.

Source event duration (t_{ed}) could be on the order of $(\frac{X}{V_{cr}})$ where 'X' is the distance moved by the crack and 'V_{cr}' the velocity with which crack is moving. In case of cementitious materials, cracks propagate at several meters per second, giving ample spectral content up from zero and up through the ordinary AE frequency range. The documented cases for the velocities of fast-running

cracks are generally for metals, glass (Pollock, 1981). But given the nature of the stiff and brittle constituent materials (or coarse aggregates), velocities on this same order would be the case for cracks in concrete also. To illustrate this, curves of cumulative hits versus AE energy during the compressive fracture process are shown in Fig. 14a – Fig. 14c respectively.

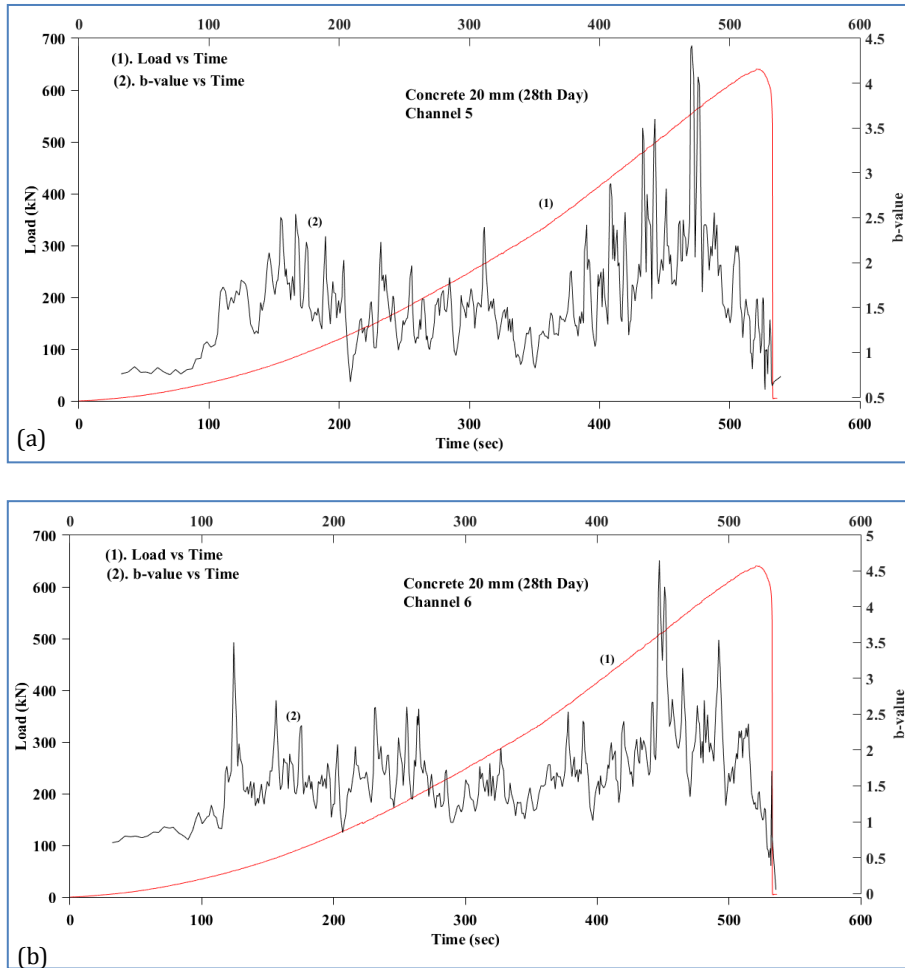


Fig. 11. Variation in AE based *b*-value with time and load: (a) Ch-5; (b) Ch-6.

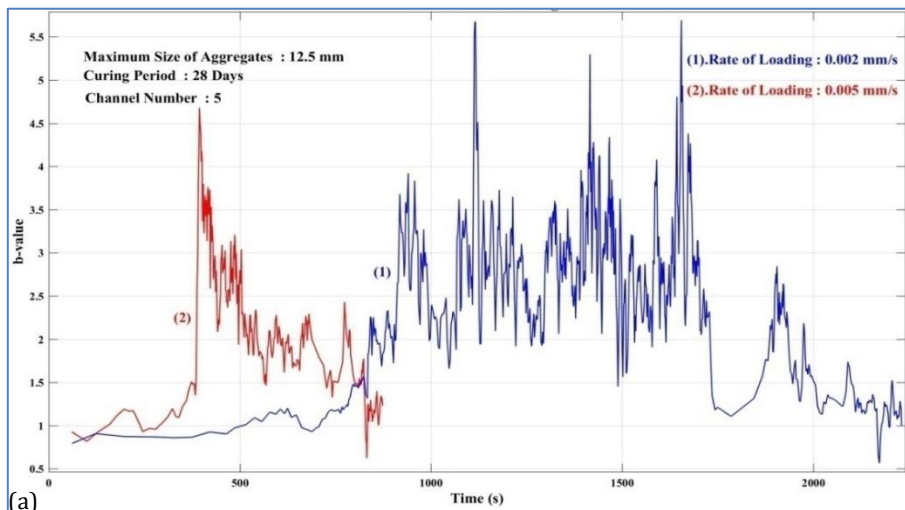


Fig. 12. (continued)

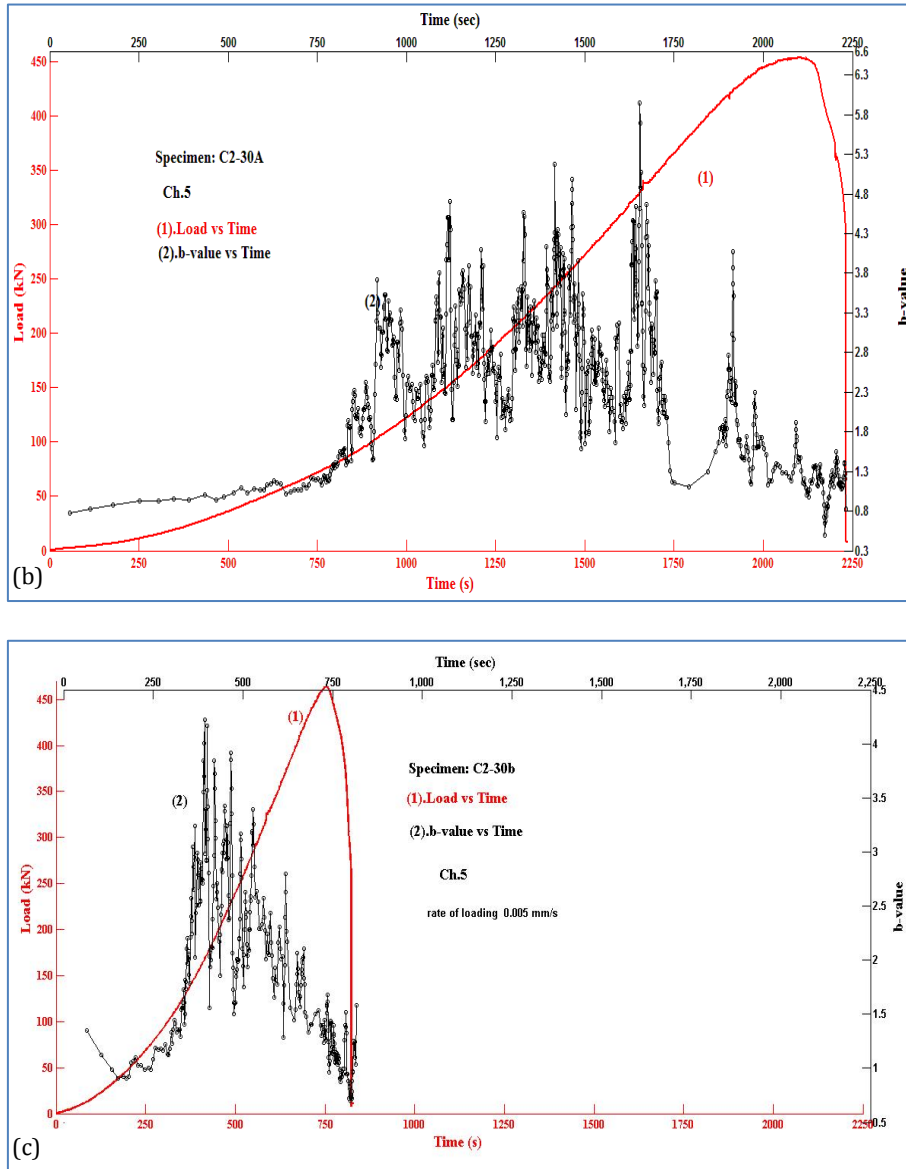


Fig. 12. Influence of loading rate on: (a) AE based *b*-value; (b) Specimen tested with 0.002 mm/s (c) specimen tested with 0.005 mm/s.

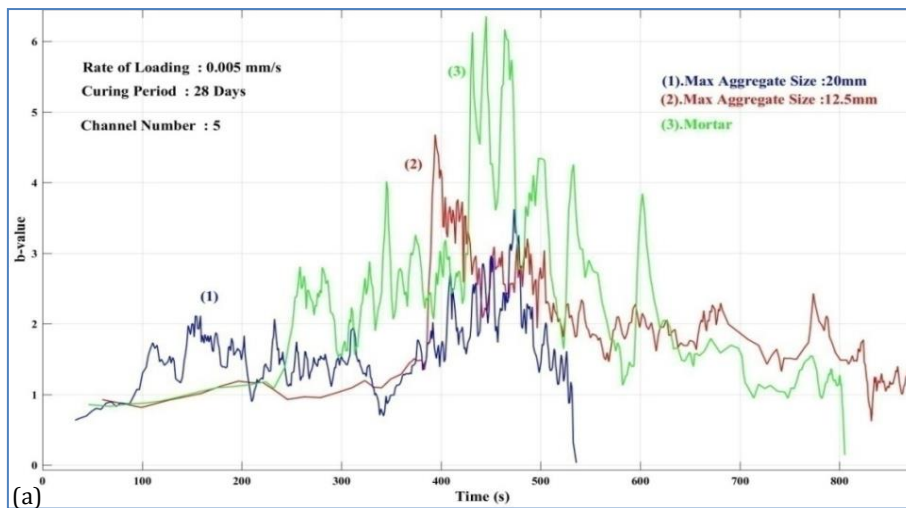


Fig. 13. (continued)

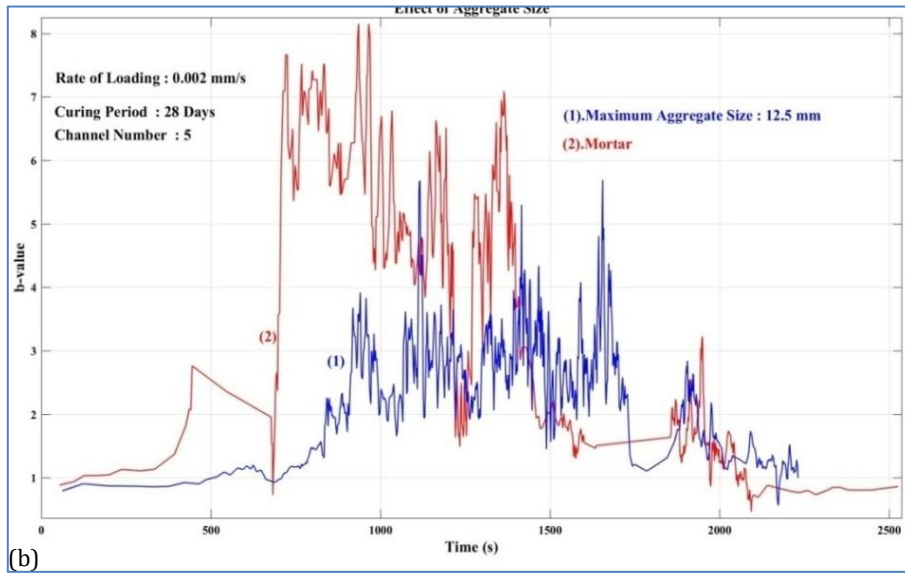


Fig. 13. AE based *b*-value variation in: (a) concrete-I and mortar; (b) concrete-II and mortar.

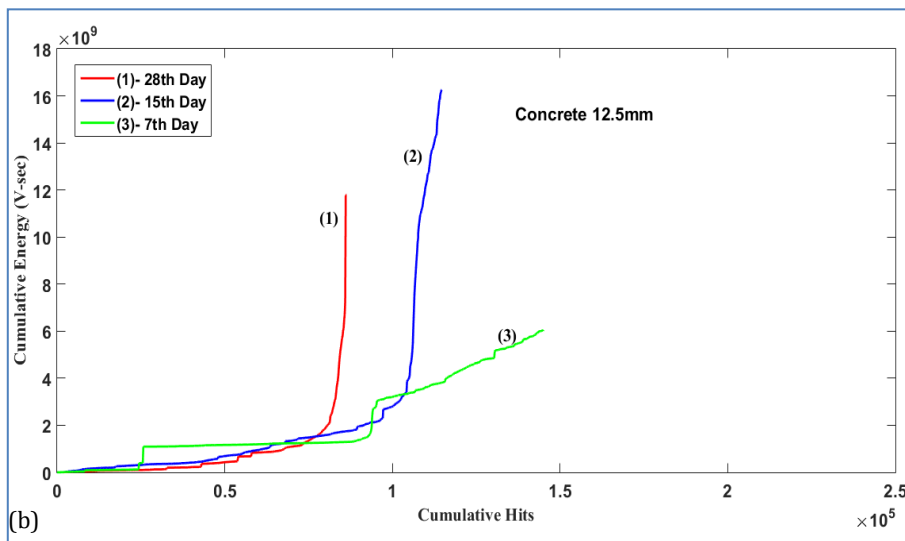
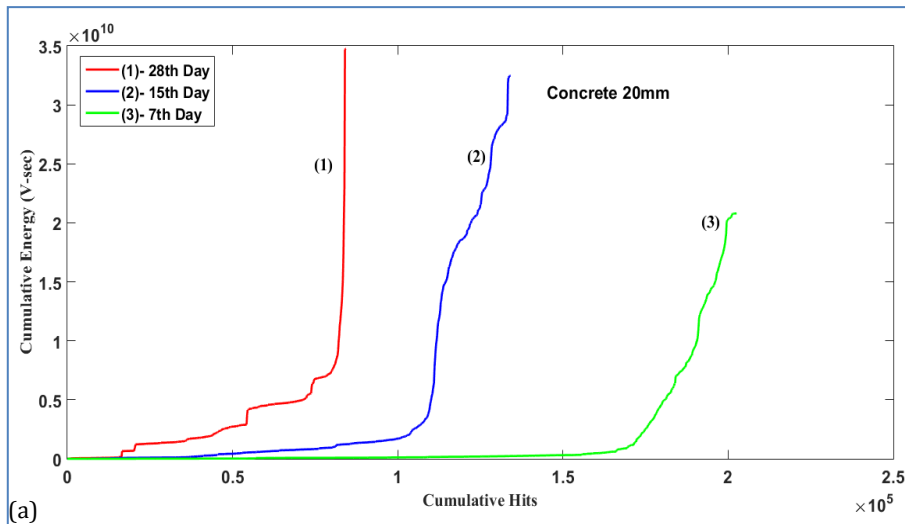


Fig. 14. (continued)

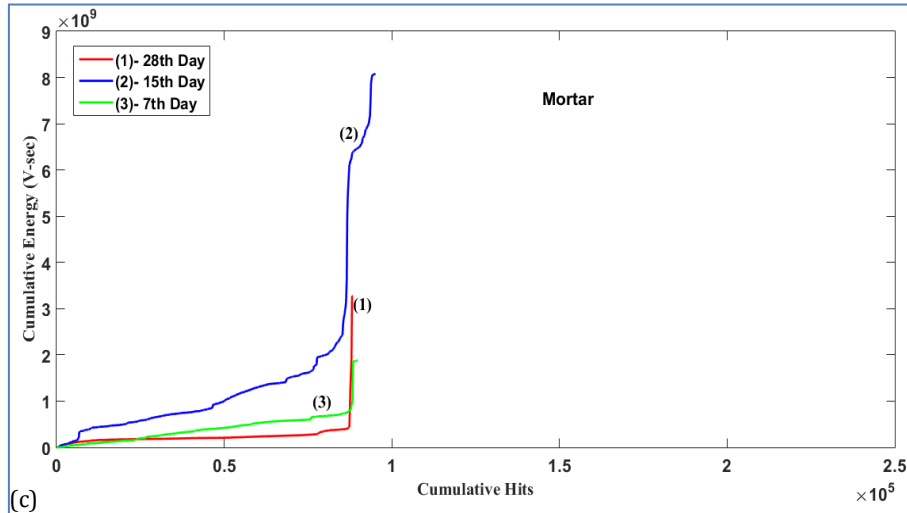


Fig. 14. Variation of AE hits released under uniaxial compressive load: (a) Concrete-I; (b) Concrete-II; (c) cement mortar.

From Fig. 14, it is observed that the number of AE hits recorded is different in the three cementitious materials. The energy released also different. As the toughness of the material is increasing the energy released is decreased. Because the coarse aggregate size in concrete

might influence the AE released as shown in Fig. 14. The fracture process of coarse aggregate might be different from cement matrix cracking because of the higher compressive strength and homogeneity of the aggregate.

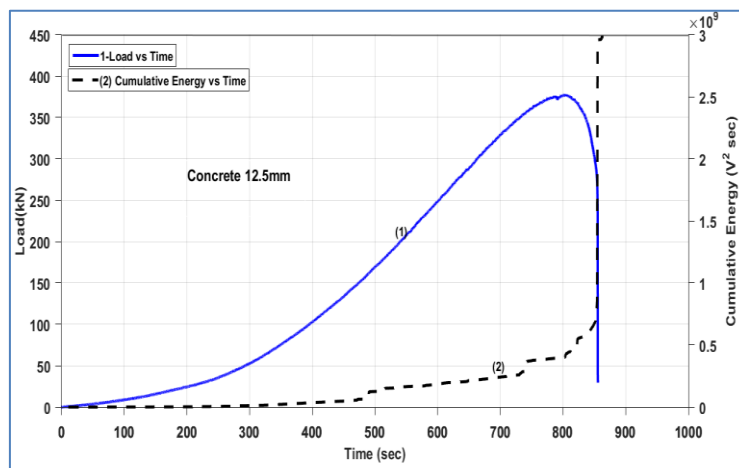
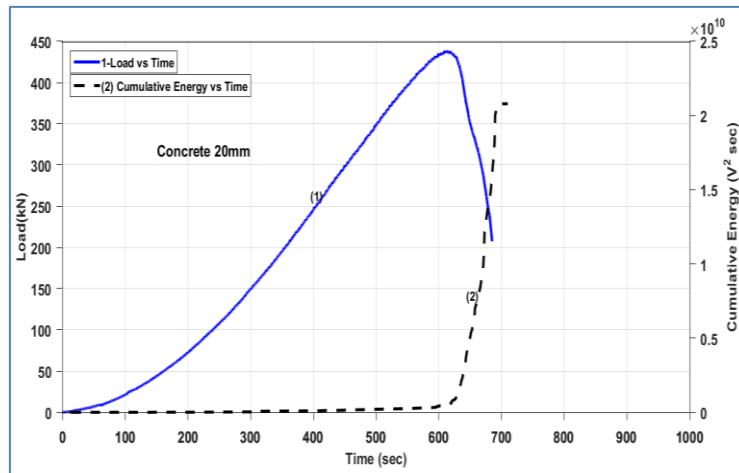


Fig. 15. (continued)

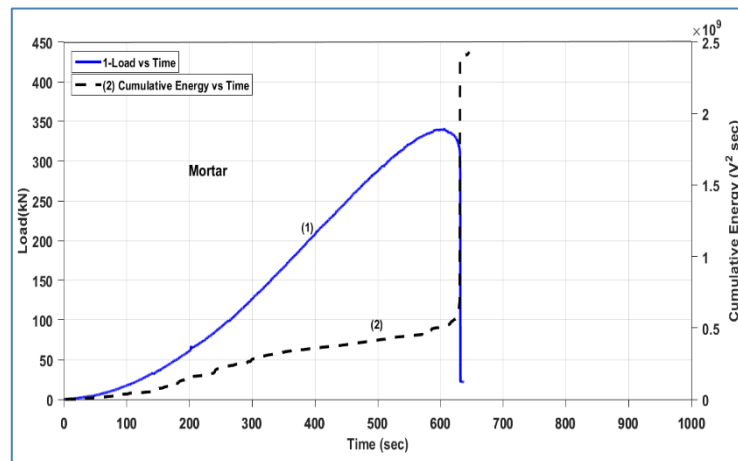


Fig. 15. Variation of AE cumulative energy released with uniaxial compressive load: (a) Concrete-I; (b) Concrete-II; (c) cement mortar.

Fig. 15, shows the AE energy released during the compressive fracture process in the three different cementitious materials. First observation is a very small AE activity occurs before peak load. From Fig. 15, one can observe that the jump in AE energy release occurs at or near peak load in Concrete-I. It indicates the onset of critical crack growth. Second observation is, AE energy release rate (the slope of the cumulative AE energy plots of Fig. 15) is greatest at the peak load, perhaps indicating that the strain energy released is maximum at this point. Also there is a taper in the AE energy release rate that occurs at before the pre-peak. While the mortar exhibits less, it is very evident in both in concrete-I and concrete-II specimens. Perhaps this suggests that the AE source mechanisms are different between the mortar and the concretes in the pre-peak region (Landis and Baillon, 2002). The reason might include the mobilization of friction, bridging, and other energy dissipation mechanisms in cementitious materials. When observed the 'AE frequency spectrum' as opposed to the 'AE source spectrum', the effects of attenuation come into it. The frequency spectrum of an electrical signal is the distribution of the amplitudes and phases of each frequency component against frequency. AE are the transient elastic waves within a material, caused by the release of localized strain energy. An event source is the phenomenon which releases elastic energy into the material, which then propagates as an elastic wave. The spectrum of the "AE wave energy" change as it propagates, with 'material absorption', away from the source. This will certainly be important when it comes to working up procedures for using AE testing on large concrete structures in-situ. Because it assumes that the frequency (f) dependent attenuation will be due to material absorption and thus proportional to AE signal frequency (f). Considering the inhomogeneity of cementitious material (aggregate-related), that this proportionality relationship will apply. Rayleigh scattering may also come into it at higher frequencies. The relationship between attenuation coefficient and frequency is likely to be different depending on whether the wavelength (λ) is greater than or less than the coarse aggregate size. The relation between wave frequency and velocity is given in Eq. (2).

$$V = f\lambda \quad (2)$$

In Eq. (2), V is the velocity, f is frequency and λ is wave length. Generally AE due to fracture process in cementitious materials is in the range of 100 kHz to 1000 kHz (Landis and Baillon, 2002). For a typical AE velocity in concrete of 4,100 m/s, a wavelength of 20 mm would correspond to a frequency of 205 kHz, which is within the frequency ranges of AE signals in concrete. For a frequency range of 100–500 kHz, the corresponding wavelengths are 40 mm–8 mm, respectively. Thus both concrete-II (coarse aggregate size 12.5 mm) and concrete-I (coarse aggregate size 20 mm) have aggregates in this regime of ultrasonic scattering. This ultrasonic scattering causes additional signal attenuation. Also material absorption takes place. Therefore reduce the total elastic wave energy that reaches the AE sensors. Due to the attenuation of AE reaching the AE sensor will be different in cementitious materials. Because, when compared with concrete-I, the coarse aggregate size is different in concrete-II and cement mortar. Hence the material absorption of the AE is different. Therefore the release of AE energy is different as shown in Fig. 15.

7. Conclusions

Based on the above experimental results, the given below major conclusions can be drawn:

- Determination of b -value using the G-R relationship is useful to study the fracture process in cementitious materials. The AE based b -value is closely related to the formation and propagation of cracks in the damage process of concrete and it decreases rapidly before the test specimen is reaching to peak load.
- AE based b -value at stresses close to failure clearly indicated the onset of 'unstable cracking' as well as 'crack coalescence' leading to dynamic failure of the cementitious materials.
- Since the AE peak amplitudes influences AE based b -value, it will be useful to examine the link between attenuation, propagation distance, frequency of sensor and b -value. Such an attempt is required for the studies on cementitious materials.

- When the compression toughness of the cementitious material increases, higher b -values are observed.
- Quick cracking occurred and lower b -values were observed, when the loading rate is high.
- As the coarse aggregate size in the cementitious material increases, the cumulative AE energy is higher. This may be due to toughness of the cementitious material.

The present study, is related to the influence of the coarse aggregate size in cementitious materials on AE peak amplitude distribution. Although water/cement ratio and cement quantity are different in the mixtures, the present study is limited to only coarse aggregate size influence of AE based b -value. Future work should investigate the variation of AE based b -value for changes in toughness and ductility of cementitious materials under uniaxial compression.

Appendix A.

A.1. Gutenberg-Richter (G-R) empirical relation

It is known from the principles of seismology that the earthquake events of larger magnitude occur less frequently than the events of smaller magnitude. This observation in seismology is known as the Gutenberg-Richter (G-R) law (Gutenberg and Richter, 1954).

$$\log_{10}N(M) = a - bM. \quad (A1)$$

G-R law given in Eq. (A1) is an empirical relation between the magnitude and total number of earthquakes occurred in a given region during a specific time interval. G-R law represents the cumulative distribution function (CDF) of seismic events using a frequency-magnitude relation. In Eq. (A1), M is the Richter magnitude of earthquakes. It is the logarithm of the integral of slip along the fault during an earthquake. $N(M)$ is the total number of earthquakes of magnitude greater than M .

$$N(M) = \int_M^{\infty} n(M)dM. \quad (A2)$$

In other words, $N(M)$ is the number of earthquake events having a magnitude M occurred during a specific time interval in a particular region. 'a' and 'b' are empirical constants. The constant 'a' is dependent on the seismicity rate which varies from region to region. The constant 'b' is the b -value. In fact, b -value is the slope of the amplitude CDF. In Eq. (A1), the b -value is the negative gradient of the log-linear plot of earthquake occurrences and the corresponding magnitudes. In Eq. (A2), $n(M)$ is the number of earthquakes of magnitude M . $N(M)$ can be found by integrating $n(M)$ with respect to M over a range of M to ∞ .

A.2. Analogy between earthquake occurrences and acoustic emissions released during fracture in solids

Similar to the occurrence of earthquakes, during fracture process in solids, higher amplitude AE events occur less in number, and lower amplitude AE events occur

more in number. Researchers implemented G-R law to the AE peak amplitude distribution data to study the scaling of AE.

A.3. Decibel

Generally, decibel (dB) describes a ratio. The dB is a logarithmic way of describing a ratio. If the ratio is related to voltage

$$dB = 10 \log_{10} \left[\frac{V_p}{V_{ref}} \right]^2, \quad (A3)$$

where V_p is the peak signal voltage in micro-volts referred to the pre-amplifier input. In general, $(dB)_{AE}$ is used for measurement of AE signal peak amplitude A . From Eq. (A3) AE peak amplitude in decibels can be written as

$$A_{dB} = 10 \log_{10} \left[\frac{A_{max}}{A_{ref}} \right]^2, \quad (A4)$$

$$A_{dB} = 20 \log_{10} \left[\frac{A_{max}}{A_{ref}} \right]. \quad (A5)$$

A.4. Earthquake magnitude and amplitude

From Eq. (A1) one can write

$$M = \frac{a - (\log_{10}N)}{b}. \quad (A6)$$

From Eq. (A6) and Eq. (A2), it can be observed that the earthquake magnitude is proportional to the logarithm of the maximum amplitude. Because Richter magnitude scale assigns a magnitude number to quantify the size of an earthquake. Therefore earthquake magnitude (M) is determined by measuring the amplitude of the largest wave (A_{max}) recorded on the seismogram. Hence

$$M \propto \frac{2}{3} c \log_{10} A_{max}, \quad (A7)$$

where c refers to the time constant of the transducer and the associated circuitry. Substituting Eq. (A7) into Eq. (A1). Here earthquake magnitude M is analogous to AE signal peak amplitude, A_{max} . AE magnitude, which has no units is computed using the amplitude data (units: dB or volts).

$$\log_{10} N(M) = a - b_{AE} [20 \log_{10} A_{max}] [A_{ref}=1]. \quad (A8)$$

A.5. Comparison of M and amplitude of AE event

Comparing M values both in case of earthquake phenomenon and acoustic emission phenomenon.

In case of earthquakes, M value for Eq. (A1) is given in Eq. (A7). In case of acoustic emission: M value is given in Eq. (A8).

From Eq. (A1) and Eq. (A8).

$$20 b_{AE} \log_{10} A_{max} = b \frac{2}{3} c \log_{10} A_{max}, \quad (A9)$$

Considering AE transducer is a velocity transducer (Colombo et al., 2003) and assuming 'c' is equal to 1.5. Eq. (A9) becomes

$$20b_{AE} = b \frac{2}{3} c, \quad (A10)$$

$$b_{AE} = \frac{b}{20}, \quad (A11)$$

$$\log_{10} N(A) = a - b_{AE} [A_{dB}]. \quad (A12)$$

Therefore, G-R law given in Eq. (A1) is modified to implement for AE testing is given below.

$$\log_{10} N(A) = a - b \left[\frac{A_{dB}}{20} \right]. \quad (A13)$$

where A_{dB} is the peak amplitude of the AE hits (or events) in decibels. b is the AE-based b -value. $N(A)$ is the number of AE hits of amplitude greater than or equal to A . 'a' is constant. The constant 'a' is determined mostly based on surrounding noise of the test area. Therefore to use the same G-R law given in Eq. (A1), one should divide acquired AE peak amplitudes by 20. Because AE peak amplitude recorded is in dB units and Richter magnitude of earthquakes defined in terms of logarithm of maximum amplitude.

REFERENCES

- Carpinteri A, Lacidogna G, Pugno N (2006). Richter's laws at the laboratory scale interpreted by acoustic emission. *Magazine of Concrete Research*, 58(9), 619-625.
- Colombo IS, Main IG, Forde MC (2003). Assessing damage of reinforced concrete beam using b -value analysis of Acoustic emission signals. *Journal of Materials in Civil Engineering*, 15(3), 280-286.
- Grosse C, Ohtsu M (2008). Acoustic Emission Testing. Berlin, Springer-Verlag, Heidelberg.
- Gutenberg B, Richter CF (1954). In Seismicity of the Earth and Associated Phenomena, Princeton University Press, Princeton, NJ, USA, 2nd Ed.
- Holford KM (2000). Acoustic emission - Basic principles and future directions. *Strain*, 36(2), 51-54.
- Ko W, Yu C (2009). Application of Gutenberg Richter Relation in AE Data Processing. *International Journal of Applied Science and Engineering*, 7(1), 69-78.
- Kalyanasundaram P, Mukhopadhyay CK, SubbaRao SV (2007). Practical acoustic emission. Narosa Publishing House private limited, New Delhi.
- Kurz JH, Finck F, Grosse CU, Reinhardt HW (2006) Stress drop and stress redistribution in concrete quantified over time by the b -value analysis. *Structural Health Monitoring*, 5, 69–81.
- Landis EN, Baillon L (2002). Experiments to Relate Acoustic Emission Energy to Fracture Energy of Concrete. *Engineering Mechanics*, 128(6), 698-702.
- Mogi K (1962) Magnitude–frequency relation for elastic shocks accompanying fracture of various materials and some related problems in earthquakes. *Bulletin of Earthquake Research Institute, Tokyo University*, 40, 831–853.
- Mehta PK, Monteiro PJM (2006) Concrete: Microstructure, properties and materials. McGraw-Hill, Third edition.
- Nair A, Cai C (2010). Acoustic emission monitoring of bridges: Review and case studies. *Engineering Structures*, 32(6), 1704-1714.
- Neville AM (2011). Properties of Concrete. Pearson Education Limited, Edinburgh Gate Harlow Essex CM20 2JE England.
- Ohtsu M (1998). Basics of acoustic emission and applications to concrete engineering. *Materials Science and Research International*, 4(3)131-140.
- Pollock AA (1981). Acoustic emission amplitude distributions. *International Advances in Nondestructive Testing*, 7, 215-239.
- Datt P, Kapil JC, Kumar A (2015). Acoustic emission characteristics and b -value estimate in relation to waveform analysis for damage response of snow. *Cold Regions Science and Technology*, 117, 170-182.
- Rao MVMS, Prasanna Lakshmi KJ (2005). Analysis of b -value and improved b -value of acoustic emissions accompanying rock fracture. *Current Science*, 89, 1577-1582.
- RILEM TC 212-ACD (2010a). Acoustic emission and related NDE techniques for crack detection and damage evaluation in concrete. Measurement method for acoustic emission signals in concrete. *Materials and Structures*, 43(9), 1177-1181.
- RILEM TC 212-ACD (2010b). Acoustic emission and related NDE techniques for crack detection and damage evaluation in concrete. Test Method for damage qualification of reinforced concrete beams by AE. *Materials and Structures*, 43(9), 1183-1186.
- RILEM TC 212-ACD (2010c) Acoustic emission and related NDE techniques for crack detection and damage evaluation in concrete. Test method for classification of active cracks in concrete structures by acoustic emission. *Materials and Structures*, 43(9), 1187–1189.
- Proverbio E (2011). Evaluation of deterioration in reinforced concrete structures by AE technique. *Materials and Corrosion*, 62(2), 161-169.
- Schumacher T, Higgins CC, Lovejoy SC (2011). Estimating operating load conditions on reinforced concrete highway bridges with b -value analysis from acoustic emission monitoring. *Structural Health Monitoring*, 10(1), 17-32.
- Shiotani T, Yuyama S, Li Z, Ohtsu M (2001). Application of AE improved b -value to quantitative evaluation of fracture process in concrete materials. *Journal of Acoustic Emission*.
- User's Manual. AE^{win} SAMOS Software (2004). Physical Acoustics Corporation, Princeton Jct, NJ, USA.
- Uchida, M, Okamoto T, Ohtsu M (2011). Damage of reinforced concrete qualified by AE. *Challenge Journal of Concrete Research Letters*, 2(3), 286-289.
- vanMier JGM (1997). Fracture Process of Concrete. Assessment of material parameters for fracture models. CRC Press.
- vanMier JGM (1998). Failure of concrete under uniaxial compression: An overview. *Proceedings of the 3rd International conference on Fracture mechanics of concrete and concrete structures (FraMCoS-3)*, Gifu, Japan, AEDIFICATIO, Freiburg, Germany, 1169-1182.
- Vidya Sagar R, Rao MVMS (2014). An experimental study on loading rate effect on acoustic emission based b -values related to reinforced concrete fracture. *Construction and Building Materials*, 70, 460-472.